Finite Element Analysis of Cooling Time and Residual Strains in Cold Spray Deposited Titanium Particles

Thanh-Duoc Phan, Saden H. Zahiri, S. H. Masood, Mahnaz Jahedi

Abstract—In this article, using finite element analysis (FEA) and an X-ray diffractometer (XRD), cold-sprayed titanium particles on a steel substrate is investigated in term of cooling time and the development of residual strains. Three cooling-down models of sprayed particles after deposition stage are simulated and discussed: the first model (m1) considers conduction effect to the substrate only, the second model (m2) considers both conduction as well as convection effect to the environment, and the third model (m3) which is the same as the second model but with the substrate heated to a near particle temperature before spraying. Thereafter, residual strains developed in the third model is compared with the experimental measurement of residual strains, which involved a Bruker D8 Advance Diffractometer using CuKa radiation (40kV, 40mA) monochromatised with a graphite sample monochromator. For deposition conditions of this study, a good correlation was found to exist between the FEA results and XRD measurements of residual

Keywords—cold gas dynamic spray, X-ray diffraction, explicit finite element analysis, residual strain, titanium, particle impact, deformation behavior.

I. INTRODUCTION

TECHNOLOGICAL advantages of titanium make this material attractive for a range of applications including aviation, sports, medical devices, and automotive industry. However, application of titanium is limited due to the high costs for producing and machining; where cost for titanium is approximately ten times more than steel. Improvement in fabrication process for titanium is fundamental for more cost effective titanium products in the future.

Cold spray technology offers a cost-effective alternative for a wide range of products including titanium. In this technology, titanium particles in a carrier gas are accelerated under high pressure and temperature using a De Laval type nozzle to supersonic velocity (~500-1000 m/s) [1]. The impact of particles to substrate results in plastic deformation and bonding, which create coatings. Compared with other spray technologies, cold spray process temperatures during the impact is generally below the melting temperature of particles. This, under certain conditions, has the potential to produce an oxygen free deposit [2].

- T. D. Phan is with Swinburne University of Technology, *Hawthorn, Vic.* 3122, *Australia* (e-mail: Dphan@swin.edu.au).
- Dr S. H. Zahiri is with CSIRO Manufacturing and Materials Technology, Gate 5, Normanby Road, Clayton, Vic. 3168, Australia (e-mail: Saden.Zahiri@csiro.au).
- Prof S. H Masood is with Swinburne University of Technology, Hawthorn, *Vic 3122, Australia* (e-mail: SMasood@swin.edu.au).
- Dr M. Jahedi is with CSIRO Manufacturing and Materials Technology, Gate 5, *Normanby Road, Clayton, Vic. 3168, Australia* (e-mail: Mahnaz.Jahedi@csiro.au).

Finite element method allows high velocity impact behavior of particles to be simulated and visualised. It helps to investigate the effects of varying coating conditions to the characteristics of sprayed titanium parts. Recently, Zhang, Li and Liao [3] have modelled the impact and deformation behaviors of spray particle. The reported numerical results have indicated that the flattening ratio of particles increases with the increase in particle impact velocity, which is comparable to other published work [4, 5].

The finite element method can also be applied to determine residual strains in coatings [6, 7], which is an important parameter in a cold spray process because failure of coating due to residual strains is a serious problem like cracking. Predicting the development of residual strains can also help to avoid strain-induced failures. Ghafouri-Azar et. al. [8] investigated the effect of varying both substrate and coating temperature on development of residual strain. In their study, a high velocity oxy-fuel torch was used to deposit coating of both stainless steel and tungsten carbide cobalt alloy on a stainless steel substrate.

In addition, measurement of residual strain by X-ray diffraction (XRD), which is a non-destructive method, has been widely used to investigate the development of residual stress and strain by several researchers [7, 8]. In the measurement process, mono-chromised X-ray is diffracted following Bragg's law [9]:

$$n.\lambda = d.\sin(2\theta) \tag{1}$$

where n = order of magnitude, λ = X-rays wavelength, d = lattice spacing and 2θ = diffraction angle.

Any strain in the material causes the planes in the crystal lattice to change and a tilt in reflected beam occurs from the original with a slightly different angle. A diffraction peak is made up of many peaks from different sub-grains. Their shape depends on crystal size, and their position on the local microstrain [10]. For example, shifted planes create smaller diffraction peaks around the original one resulting in so called "X-ray Line Broadening". All single peaks together solve in the measured diffraction peak [11].

In this study, cold-sprayed titanium particles on a steel substrate are analysed in term of cooling time and developed residual strains using the finite element analysis (FEA) and X-ray diffractometer (XRD) measurement. Three types of cooling-down models of sprayed particles after deposition

stage are considered and discussed. The first model (m1) is the model with conduction effect to the substrate only, the second model (m2) is the model with the condition of conduction plus convection effect to the environment. Lastly, the third model (m3) is the same as the second model added the substrate surface was heated to a near particle temperature before spraying. Thereafter, the closest to reality model, which is the m3 model, was chosen to carry out further investigation on the development of residual strains.

II. MODELLING AND SIMULATION OF PARTICLE DEFORMATION AND COOLING PROCESS

Explicit impacting behavior and cooling time of a single titanium (Ti) particle sprayed on steel substrate was modeled using a commercial FEA program with an initial assumed temperature and velocity of 690°C and 770m/s respectively. The substrate surface is also assumed to be flat with zero roughness, and particles are in spherical shape.

The impact was defined as a nonlinear dynamic contact. The particle and substrate interaction was implemented by using the body penalty formulation. The material deformation was described by the Johnson and Cook plasticity model [8], which accounts for strain hardening, strain rate hardening, and thermal softening effects. The plasticity dynamic failure model is based on the value of the equivalent plastic strain at element integration points, where failure is assumed to occur when the damage parameter exceeds. The most important aspect of the simulations on Lagrangian algorithm is the possible excessive distortion of elements near the contact surfaces. To overcome this, the element distortion control and adaptive meshing techniques were utilized. Using all of the above parameters, residual strains were then estimated from the Lagrangian formulation, which has been used in several numerical and simulation models [9, 10].

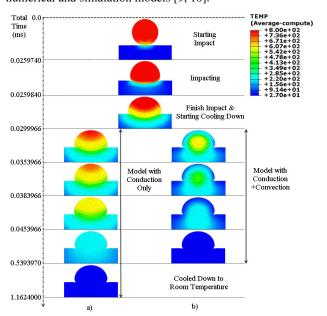


Fig. 1 Temperature contours of deformed Ti particles during cooling stage of models m1 (a) and m2 (b)

As mentioned before, there were three FEA models simulated for comparison during cooling down process. All of the models are similar in their materials, geometric dimensions, ambient temperatures, velocity of impingement, and heat loads. The first model (m1) takes into account of cooling by conduction only. The second simulation (m2) considers conduction plus convective air cooling. Lastly, the model (m3) has the same conditions as the second model with the only difference is that steel substrate was heated to a near particle temperature before spraying. Fig. 1 shows the temperature distributions of the deformed titanium particles during the cooling stage of the first two models.

As illustrated in Fig. 1, the explicit dynamic analysis was run and finished normally after approximately ~1.1624ms and 0.539397ms for the first and second models respectively. The cooling rate is faster when both conduction and convection effects are considered in m2 model. In other words, with adding the convective air cooling around, the deposited particle was cooled down to room temperature after 0.5394ms, which is almost 55% faster cooling compared to the conductive only model (m1). The second model also gave a more plausible result, which had the hottest spot moving down to the particle/substrate interface, whereas the hottest spot remains at the particle top-node for the first model, which is basically not accurate.

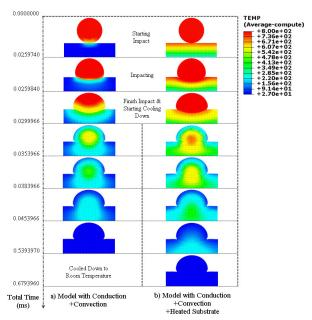


Fig. 2 Temperature contours of deformed Ti particles during cooling stage of m2 (a) and m3 (b)

Similarly, Fig. 2 shows the comparisons of deformation and temperature contours of particles during the cooling stage in the second and the third model. It can be seen after impingement that the hottest spot is occurred at the point of contact between particle and substrate in both cases. However, the interface remains hot for a longer time when the pre-heated substrate condition was considered in the later

model which is m3. As expected, the total cooling time of the m3 model 0.6794ms was higher than that of the m2 model, which is 0.5394ms.

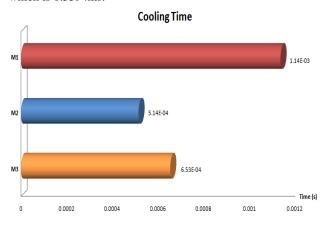


Fig. 3 Cooling time for all three models

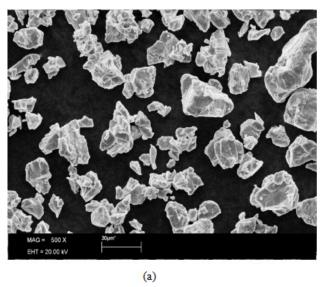
For comparison purposes, Fig. 3 shows the total cooling times for all three simulated models: (m1) involving only conduction at the interface, (m2) involving conduction at the interface and convection to air, and (m3) involving conduction at the interface plus convection to air and also with the substrate heated to near particle temperature before impact. It reveals that the conduction and convection model m2 has the fastest cooling rate, which is 55% faster than the model with only conduction (m1), and is also 20% faster than the model with heated substrate (m3). From a practical point of view, the m3 is the most convincing model that demonstrates the characteristics of cold spray process, in which the substrate top surface always gets heated to a temperature by the hot spraying gas.

III. EXPERIMENTAL STRESS/STRAIN MEASUREMENT

In this section, residual strains obtain from simulation results are compared with experimental residual strain measurements using X-ray diffraction. Firstly, in order to create a Titanium coating on an iron tube, A CGTTM KINETIKS® 4000 system was used with nozzle body attached to a robot. Nitrogen was used as carrier gas for powder with gas quantity of 2.8m³/h. The powder used was commercially pure titanium (CP Ti) of ASTM Grade 4.

TABLE I ELEMENTAL ANALYSIS OF USED POWDER

Element	Ratio (%)
Ti Si O	Balance 0.9 0.35
C H N Fe Other	0.03 0.01 0.00016 0.4 max



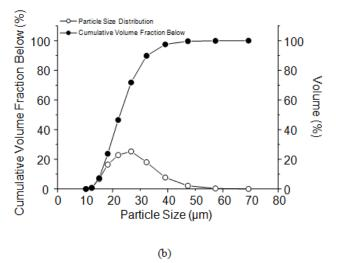


Fig. 4 (a) Scanning electron microscopy images, and (b) Size distribution of the CP titanium powder used for testing with $27\mu m$ mean diameter

Fig. 4 shows the scanning electron microscopy image of the particles and the size distributions of the used CP titanium powder which has the average particle size of $27\mu m$.

The powder was fed at powder feeder disc rotation of 2.5 rpm. A iron rod (S316, 300mm, Ø16mm) was used as a substrate. To ensure a uniform coating thickness, substrate was rotated at 300 rpm during the spray process. The robot was programmed to rapidly move the nozzle from a starting position, 100mm above the sample, down to the spray position, 35mm away from the rotating rod. After 1s, nozzle moved rapidly back to the starting position to finish one spray pass. The gas temperature and pressure in the nozzle were constant at 800°C and 30 [bar] respectively to ensure high deposition efficiency. After the deposition process, the sample cooled down to room temperature, and the coating was formed as expected with a measured thickness of approximate 250µm.

Using a Bruker D8 Advance Diffractometer, the Ti-coating was scanned over the 2-theta range of 30° to 90° with an inclination of 0.02° and a count time of 6s per step, as shown in Fig. 5. The results were then analysed using the search match program EVATM and the ICDD-JCPDS database for crystal phase identification.

During the measurement process, there was a problem in which the incoming X-ray had to hit the sample exactly in the middle; otherwise the cylindrical shape of the rod would cause a ψ angle other than zero. That means the sample had to be fixed at the correct height, otherwise the diffraction plot shows only back reflection (sample too low) or peaks at a lowered angle (sample too high).

However, with the help of the front sample guiding pin, the correct sample position could be transferred to the titanium coatings. The dominating Ti 101 peak was used to align the coatings under the beam focus. Over a 2-theta range from 38° to 41° with a step size of 0.02° and a step time of 0.5s, the correct focus point was established while the sample was adjusted by raising or lowering the laboratory jack. Interestingly, as also shown in Fig. 5, the sample produces diffraction peaks for both titanium (red line) and iron (green

line), which should not have occurred, as maximum XRD-beam penetration for current experiment is expected to be in the range of 3.2 μm to 8.7 μm . One explanation for this may be due to the presence of porosity in thin titanium coating (~250 μm), which allows for X-ray beam to reflect from the stainless steel tube surface. Consequently, a retort stand and a clamp were used to fix the sample under the beam focus. To determine the correct adjustment, the diffraction maximum of the steel bar (110-Fe-peak at 20 \approx 44.731°) was identified. The Bruker TOPASTM software was also used to fit the peaks in a pseudo-Voigt function, from that the average Gaussian strain in the coating surface was then calculated to be $\epsilon XRD \approx 0.140$.

On the other hand, Fig. 6 shows the results obtained from the simulation of the third model which had heated substrate plus conduction and convection effects during cooling down stage. The contours show that particle flattened after impact with the highest residual compressive strain of 0.603. Generally, strain near the interface was higher than those near the free surface. Most of the particle elements are highly strained apart from the deformed area near the surface of the substrate, and the substrate also bears some of the strains.

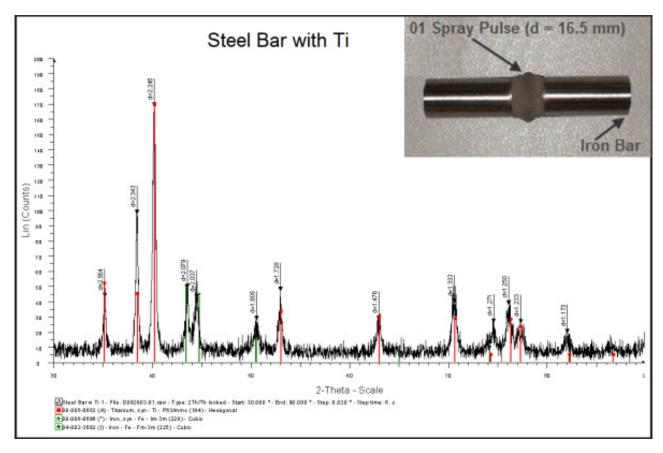


Fig. 5 X-ray diffraction plot of the Ti coating on an iron tube

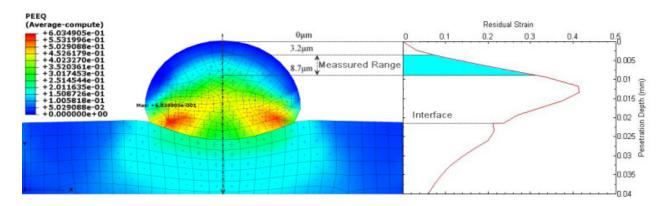


Fig. 6: Calculated residual strain of single particle for the heated substrate model (m3).

Fig. 6 also shows that the average straining that occurs along the vertical direction, within the range of 3.2µm to 8.7µm from the top of particle, is ϵ FEA \approx 0.165457, which is in close agreement with the XRD result (ϵ XRD \approx 0.14). The difference in the results may be caused by the fact that the titanium particles used in the experiment were not spherical as well as due to some other assumptions made such as zero-roughness substrate surface and assumed value calculations of particle temperature and velocity.

IV. CONCLUSION

This study considers the convection cooling and substrate pre-heating effects as important events for estimating temperature history and residual strain in titanium cold spray process. Deformation, cooling time and residual strain in all three simulated models was estimated and compared. The results show that finite element analysis and X-ray diffraction outcomes are in agreement in respect to the straining that occurs on the outer surface of a 27µm titanium particle after deposition. In addition, when comparing the results from all three simulated models, it is found that the effects of convective air cooling and pre-heated substrate are very important. If they are included in the modeling, such as in model m3, a better and more reasonable result in term of estimating temperature history and residual strains are obtained when compared to experimental result.

REFERENCES

- S.H. Zahiri, W. Yang and M. Jahedi, J. Therm. Spray Technol., Vol. 18(1) (2009), pp. 110-117.
- [2] S.H. Zahiri, S.C. Mayo and M. Jahedi, Microsc. Microanal. Vol. 14 (2008), pp. 260–266.
- [3] W. Li, C. Zhang, C Li and H. Liao, J. Therm. Spray Technol., Vol. 18(5-6) (2009), pp. 921-933.
- [4] T. Schmidt, H. Assadi, F. Gärtner, H. Richter, T. Stoltenhoff, H. Kreye, and T. Klassen, J. Therm. Spray Technol., Vol. 18(5-6) (2009), pp. 794-808
- [5] D. Rafaja, T. Schucknecht, V. Klemm, A. Paul, and H Berek, Surf. Coats. Technol., Vol. 203(20-21) (2009) pp. 3206-3213.
- [6] B.D. Cullity and S.R. Stock, 3rd Edition, "Elements of X-ray Diffraction", Prentice Hall, New Jersey (2001).
- [7] I. Noyan, and J. Cohen, "Residual Strain-Measurement Diffraction and Interpretation", Springer-Verlag, (1987).
- [8] R. Ghafouri-Azar, J. Mostaghimi and S. Chandra, Comp. Mater. Sci., Vol. 35 (2006) pp. 13-26.
- [9] H. P. Klug and L. E.Alexander, "X-ray Diffraction Procedures for Polycrystalline and amorphous Materials", 2nd Edition, John Wilay & Sons, New York (1974).
- [10] K. Kim, M. Watanabe and S. Kuroda, J. Therm. Spray Technol., Vol. 18(4) (2009), pp. 490-498.
- [11] C. Lyphout, P. Nylen, A. Manescu and T. Pirling, J. Therm. Spray Technol., Vol. 17(5-6) (2008), pp. 915-923.